



**QUEEN'S  
UNIVERSITY  
BELFAST**

## **Mitigating of Arsenic Accumulation in Rice (*Oryza sativa* L.) from Typical Arsenic Contaminated Paddy Soil of Southern China Using Nanostructured $\alpha$ -MnO<sub>2</sub>: Pot Experiment and Field Application**

Li, B., Zhou, S., Long, J., Peng, L., Tie, B., Williams, P., & Lei, M. (2019). Mitigating of Arsenic Accumulation in Rice (*Oryza sativa* L.) from Typical Arsenic Contaminated Paddy Soil of Southern China Using Nanostructured  $\alpha$ -MnO<sub>2</sub>: Pot Experiment and Field Application. *Science of the Total Environment*, 650(1), 546-556. <https://doi.org/10.1016/j.scitotenv.2018.08.436>

**Published in:**  
Science of the Total Environment

**Document Version:**  
Peer reviewed version

**Queen's University Belfast - Research Portal:**  
[Link to publication record in Queen's University Belfast Research Portal](#)

### **Publisher rights**

Copyright 2018 Elsevier.

This manuscript is distributed under a Creative Commons Attribution-NonCommercial-NoDerivs License

(<https://creativecommons.org/licenses/by-nc-nd/4.0/>), which permits distribution and reproduction for non-commercial purposes, provided the author and source are cited.

### **General rights**

Copyright for the publications made accessible via the Queen's University Belfast Research Portal is retained by the author(s) and / or other copyright owners and it is a condition of accessing these publications that users recognise and abide by the legal requirements associated with these rights.

### **Take down policy**

The Research Portal is Queen's institutional repository that provides access to Queen's research output. Every effort has been made to ensure that content in the Research Portal does not infringe any person's rights, or applicable UK laws. If you discover content in the Research Portal that you believe breaches copyright or violates any law, please contact [openaccess@qub.ac.uk](mailto:openaccess@qub.ac.uk).

### **Open Access**

This research has been made openly available by Queen's academics and its Open Research team. We would love to hear how access to this research benefits you. – Share your feedback with us: <http://go.qub.ac.uk/oa-feedback>

1 **Mitigating of Arsenic Accumulation in Rice (*Oryza sativa* L.)**  
2 **from Typical Arsenic Contaminated Paddy Soil of Southern**  
3 **China Using Nanostructured  $\alpha$ -MnO<sub>2</sub>: Pot Experiment and**  
4 **Field Application**

5 **Bingyu Li<sup>abc</sup>, Shuang Zhou<sup>abcd</sup>, Dongning Wei<sup>abc</sup>, Jiumei Long<sup>abc</sup>, Liang Peng<sup>abc</sup>,**  
6 **Baiqing Tie<sup>abc</sup>, Paul N. Williams<sup>e</sup>, Ming Lei<sup>abc\*</sup>**

7 <sup>a</sup>*College of Resource & Environment, Hunan Agricultural University, Changsha*  
8 *410128, P. R. China*

9 <sup>b</sup>*Hunan Engineering Research Center for Safe and High-Efficient Utilization of*  
10 *Heavy Metal Pollution Farmland, Changsha 410128, P. R. China*

11 <sup>c</sup>*Provincial Key Laboratory of Rural Ecosystem Health in Dongting lake area, Hunan*  
12 *province, Changsha 410128, P. R. China*

13 <sup>d</sup>*Laboratory of Environmental Geology, Graduate school of Engineering, Hokkaido*  
14 *University, Kita 13 Nishi 8, Kita-Ku, Sapporo 060-8628, Japan*

15 <sup>e</sup>*Queen's University Belfast, Institute for Global Food Security, School of Biological*  
16 *Sciences, Belfast, BT9 5BN, United Kingdom*

17 *Corresponding Author at: College of Resource and Environment, Hunan Agricultural*  
18 *University, Changsha, 410128, PR China, Tel: +86 0731 84617803*

19 E-mail: [leiming@hunau.edu.cn](mailto:leiming@hunau.edu.cn) (M.Lei)\*

20 **Abstract**

21 Manganese oxides are naturally occurring powerful oxidants and scavenger  
22 which can control the mobility and bioavailability of arsenic (As). However, the effect  
23 of synthetic nanostructured manganese oxides on the mobilization and transportation  
24 of As at actual paddy soils are poorly understood, especially in the low or medium  
25 background Mn concentration soil. In the present study, a novel Nano manganese

26 oxide with higher reactivity and surface area has been synthesized. A 90-d soil  
27 incubation experiment combined with pot and field rice cultivation trials were  
28 designed to evaluate the effectiveness of exogenous  $\alpha$ -MnO<sub>2</sub> nanorods on the  
29 mobilization and transportation of As in soil-rice systems. Our results proved that the  
30 addition of  $\alpha$ -MnO<sub>2</sub> nanorods can effectively control the soil-to-solution partitioning  
31 of As under anaerobic conditions. After treatment with different amounts of  $\alpha$ -MnO<sub>2</sub>  
32 nanorods, the content of effective As decreased with the increasing of residual As and  
33 insoluble binding As (Ca-As and Fe-As). Besides, the enhanced oxidation of As (III)  
34 into As(V) by  $\alpha$ -MnO<sub>2</sub> nanorods increased the adsorption of As onto indigenous  
35 iron(hydr) oxides which greatly reduced the soil porewater As content. Additionally,  
36 pot experiment and filed applications are further proved that the influx of As into  
37 aerial parts of rice plants (stems, husk and leaves) was strictly prohibited after  
38 treatments with different amount of  $\alpha$ -MnO<sub>2</sub> nanorods; more interestingly,  
39 significantly negative correlations have been observed between As and Mn in rice,  
40 which indicated that as Mn is increased in soil, As in brown rice decreases. Our  
41 results demonstrated that the use of  $\alpha$ -MnO<sub>2</sub> nanorods in As polluted paddy soil  
42 containing low levels of background Mn oxides can be a promising remediation  
43 strategy.

44 **Keywords: Arsenic, Nanostructured-MnO<sub>2</sub>, Rice, Accumulation, Paddy soil**

## 45 **1. Introduction**

46 Hunan province is world-renowned for its luxuriant deposit of non-ferrous metal

47 ores (tungsten, bismuth, realgar) (Lei et al., 2015; Okkenhaug et al., 2012; Williams et  
48 al., 2009). In the past several decades, intensive mineral exploitation, ore extraction  
49 and refining activities have caused a large amount of toxic trace elements (Cd, Hg, Pb  
50 and As) to be discharged into farmland which has greatly affected the local soil and  
51 water environment(Li et al., 2017; Zhao et al., 2015). Among them, arsenic is a  
52 ubiquitous and highly toxic metalloid element that has caused severe contamination in  
53 Hunan province(Lei et al., 2013; Lei et al., 2015). It is reported that the  
54 arsenic-contaminated farmland in Hunan province has already seriously impaired the  
55 development of agriculture and posed a serious threat to the health of local residents,  
56 because rice is a dominant staple food (Li et al., 2016; Liao et al., 2005).

57 The existence forms (speciation) of arsenic may be more important than the total  
58 arsenic in the soil, which determine its effectiveness and toxicity to organisms. It is  
59 generally established that trivalent As species are more toxic than their pentavalent  
60 counterparts because they binds to sulfhydryl groups(-SH), impairing the function of  
61 many proteins (Fu et al., 2016; Liao et al., 2005; Liu, 2005). In paddy soils, arsenic is  
62 predominantly present as the inorganic species arsenate and arsenite (Takahashi et al.,  
63 2004). The extent of As mobility and bioavailability in paddy soil is, in part, regulated  
64 by the type of minerals exist in the soil system and the oxidation state of As (Fendorf  
65 and Kocar, 2009; Ying et al., 2012). Generally, As(III) are far more mobile than  
66 As(V); and the relative content of arsenate and arsenite in paddy soil are primarily  
67 depending on the redox status of soil (Yamaguchi et al., 2011). Arsenate often exists  
68 in anionic forms (e.g.,  $\text{H}_2\text{AsO}_4^-$ ,  $\text{HAsO}_4^{2-}$ ) under aerobic conditions with the content

69 can account for 65-98% of total arsenic (Ohtsuka et al., 2013). On the contrary,  
70 arsenite takes an electrically uncharged molecule form( $H_3AsO_3$ ) under anaerobic  
71 reducing conditions ( $Eh < 100mV$ ;  $pH < 9$ ) (Han et al., 2011). The amount of Fe oxides  
72 in the soil plays an important role in controlling the concentration of As species in the  
73 soil solution; typically, As(V) is strongly adsorbed with metal-(oxyhydr) oxides,  
74 whereas As(III) is poorly associated with soil minerals owing to its feature of  
75 charge-neutral (Chen et al., 2006; Ehlert et al., 2014); and thus rendering it  
76 comparatively effective towards to plants uptake than the As(V) (Xu et al., 2017).  
77 However, it is well recognized that during the drastically aerobic-anaerobic transition  
78 within paddy fields, the adsorbed As will released into soil porewater (Ohtsuka et al.,  
79 2013; Xu et al., 2017). The mobilization of As in flooded paddy fields is because of  
80 two main processes. Firstly, the reductive dissolution of iron(oxyhydr) oxides have  
81 been triggered by soil flooding which caused the sorbed solid phase arsenic releasing  
82 into the liquid phase (Lemonte et al., 2017; Weber et al., 2010; Yamaguchi et al.,  
83 2011). Secondly, the adsorbed As(V) is reduced to As(III) under the reductive  
84 conditions and the latter has a greater tendency to partitioning into the liquid phase  
85 than As(V) (Liu et al., 2015; Takahashi et al., 2004). Compared with other terrestrial  
86 plant, rice (*Oryza sativa L.*) is efficient in As uptake and translocation, because of the  
87 flooded conditions and highly expressed arsenic transporter (Si transporter,  
88 aquaporins and phosphate transporters) (Ma et al., 2008; Meharg, 2004; Meharg and  
89 Jardine, 2003). Thus, effective measures must be taken to reduce the bio-availability  
90 and mobility of As(III) in paddy soil during rice cultivation.

91 In current literature, several measures have been proposed for reducing the  
92 bio-availability of As in soils, such as amendments stabilization (biochar, natural  
93 minerals, etc.) (Kumpiene et al., 2008; Li et al., 2018), electro-kinetics  
94 (Balasubramanian et al., 2009), acid flushing (Beiyuan et al., 2017; Tokunaga and  
95 Hakuta, 2002), phytoremediation (Gilloaiza et al., 2016; Jankong et al., 2007) and  
96 agronomic mitigation strategies (Limmer et al., 2018; Seyfferth et al., 2018). However,  
97 those methods are hard to meet the actual demand of paddy fields remediation. Due to  
98 either their high-cost (Liu et al., 2018), vast energy requirements (Villen-Guzman et  
99 al., 2017), or long treatment times (Wan et al., 2016); above all, high cost (or  
100 unsustainability) hinder the application of many technologies in polluted farmland  
101 (Bontempi, 2017). Chemical stabilization methods, in particular, have been widely  
102 accepted in the remediation of As-contaminated soils because they are relatively cost  
103 effective (sustainability) and easy to operate and management. Recently, engineered  
104 nanoparticles stabilizer such as zero valent iron (Gil-Díaz et al., 2017; Gil-Díaz et al.,  
105 2016) and iron phosphate (vivianite) nanoparticles (Liu and Zhao, 2007) has been  
106 proved to be an advanced environmental remediation technologies, which could  
107 provide cost-effective solutions to some of the most intractable environmental restore  
108 problems due to their large surface areas and high surface reactivity (Zhang, 2003).  
109 For the variable valence elements (As), by consideration of regulatory measures (in  
110 situ oxidation by chemical amendments) to induction the transformation of As(III) to  
111 As(V) is considered to be a promising approach which can alleviate the associated  
112 environmental risks of As in paddy soil (Lin et al., 2017; Suda and Makino, 2016; Xu

113 [et al., 2017](#)). However, to our knowledge, there are few related studies focused on the  
114 induction of As to be transformed into low-effective and low-toxicity forms using  
115 oxidants in paddy soil.

116 Manganese oxides are naturally occurring powerful oxidants that can effectively  
117 catalyze the oxidation of As(III) to As(V) under natural circumstances ([Bruce A.  
118 Manning et al., 2002](#); [Ehlert et al., 2014](#); [Han et al., 2011](#); [Lafferty et al., 2010](#)). The  
119 As(III) oxidation by manganese oxides can occur across a wide pH ranged from  
120 4.0~8.2, however, the oxidation rates are deeply associated with their structure,  
121 surface charge properties, mineral crystallinity and abundance ([Oscarson et al., 1983](#);  
122 [Scott and Morgan, 1995](#)). The study conducted by ([Bruce A. Manning et al., 2002](#))  
123 showed that As(III) can be quickly oxidized into As(V) in the presence of MnO<sub>2</sub> with  
124 only about 10% of As(III) was remained after 10 hours reaction. Besides, another  
125 profound and detailed researches conducted by Scott and Morgan ([Scott and Morgan,  
126 1995](#)) who found that birnessite ( $\delta$ -MnO<sub>2</sub>) can quickly oxidize As(III) to As(V), about  
127 80% of the reaction can be accomplished within 1h and this process was accompanied  
128 by the release of Mn<sup>2+</sup>. Apart from the oxidation ability towards to As(III) by  
129 manganese oxides, it was also reported that As(III), after being oxidized by  
130 Mn-oxides, can subsequently be adsorbed onto the surfaces of MnOOH (oxidation  
131 intermediates) and ferric-(oxyhydr) oxide ([Ehlert et al., 2014](#); [Nesbitt et al., 1998](#));  
132 thus the partitioning of As into solution was restrained. Although there are many  
133 studies ([BA et al., 2002](#); [Ehlert et al., 2014](#)) have been conducted on the oxidation of  
134 As(III) by manganese oxides, however, most of these studies are concentrated on pure

135 minerals in aqueous solution.

136 To the best of our knowledges, there are very few related studies on the  
137 oxidation of As(III) by synthetic nanostructured-MnO<sub>2</sub> in actual paddy soils;  
138 especially in the low or medium background Mn concentration soil. In China, it has  
139 been reported that the content of Mn in soil was varied between 10-5532 mg·kg<sup>-1</sup> with  
140 an average amount of 710 mg·kg<sup>-1</sup>(Liu et al., 1983). The Mn concentrations which  
141 below the average value of 710mg kg<sup>-1</sup> can be classified as low manganese soil.  
142 Recently, a soil incubation experiment conducted by Xu et al (Xu et al., 2017) showed  
143 that additions of synthetic Mn oxide (hausmannite) in low background Mn content  
144 paddy soils can effectively control the partitioning of As from solid phase to liquid  
145 phase due to the oxidation of As(III) However, they only have considered the  
146 efficiency of micrometer scale Mn oxides under the laboratory conditions but did not  
147 test it under complex field trials. Therefore, we have proposed a hypothesis that the  
148 endogenous iron oxides in paddy soil can be used to retain the oxidized As(V) after  
149 incorporation with nanostructured manganese oxides under flooded conditions,  
150 thereby reducing the bioavailability of As towards to rice. The major objectives of this  
151 present study are therefore to (i) investigated the potential of synthetic  $\alpha$ -MnO<sub>2</sub>  
152 nanorods on the control of solid to solution distribution of As under flooded  
153 conditions; (ii) determined whether synthetic  $\alpha$ -MnO<sub>2</sub> nanorods could reduce As  
154 uptake into rice grow in paddy soil with low endogenous Mn concentration at fields  
155 scales; and (iii) elucidated the associated mechanisms regarding to the reduced of As  
156 uptake by rice.



## 157 **2. Material and methods**

### 158 **2.1 Chemicals and reagents**

159 All chemicals, including manganese sulfate ( $\text{MnSO}_4 \cdot \text{H}_2\text{O}$ ), potassium persulfate  
160 ( $\text{K}_2\text{S}_2\text{O}_8$ ), ammonium phosphate ( $(\text{NH}_4)_3\text{PO}_4 \cdot 3\text{H}_2\text{O}$ ), urea ( $\text{CO}(\text{NH}_2)_2$ ), potassium  
161 carbonate ( $\text{K}_2\text{CO}_3$ ), hydrochloric acid ( $\text{HCl}$ ), nitric acid ( $\text{HNO}_3$ ) and sulfuric acid  
162 ( $\text{H}_2\text{SO}_4$ ) used in this study were of analytical grade without any further purification.  
163 The  $\alpha$ - $\text{MnO}_2$  nanorods was synthesized following the protocol previously outlined  
164 by [\(Yu et al., 2013\)](#) with minor modification; Briefly, the  $\alpha$ - $\text{MnO}_2$  nanorods were  
165 hydrothermally synthesized using a solution containing a certain amount of  
166  $\text{MnSO}_4 \cdot \text{H}_2\text{O}$  (0.3415 g, 2 mmol) and  $\text{K}_2\text{S}_2\text{O}_8$  (0.5434 g, 2 mmol), the detailed  
167 procedures can be found in supplementary material. The obtained  $\alpha$ - $\text{MnO}_2$  nano  
168 materials are a very stable black powdery solid. The powder X-ray diffraction (XRD)  
169 patterns of the obtained materials were recorded on a Bruker D8 Advance XRD  
170 diffractometer with  $\text{Cu K}\alpha$  radiation (Voltage: 40 kV; Current: 40 mA; Scanning rate:  
171  $10^\circ/\text{min}$ ). The morphologies of the samples were observed by emission scanning  
172 electron microscopy (SEM, Quanta F250, FEI, USA) Ultrapure water ( $18.2 \text{ M}\Omega \text{ cm}$ )  
173 was used in all experiments, unless otherwise stated. All experimental containers were  
174 soaked with 10%  $\text{HNO}_3$  overnight and rinsed several times with deionized water  
175 before use.

## 176 **2.2 Site characterization and soil sampling**

177 Chenzhou City lies between 24°53′ and 26°50′ latitudes and between 112°13′  
178 and 114°14′ longitudes(Lei et al., 2015). The research paddy field is located in  
179 Dengjiatang (25°36′N, 113°00′E) village, Su Xian district, Chenzhou City. An  
180 As-product factory was located at Dengjiatang in 1992, but it has been out of  
181 production since 1999(Lei et al., 2015; Liao et al., 2004; Liao et al., 2005).

182 Bulk arsenic contaminated soil samples were collected from the plow layers  
183 (0-20cm). The soil samples were air-dried at room temperature, ground, and passed  
184 through a 5-mm nylon sieve. The elementary physicochemical properties were  
185 analyzed, and the results were shown in Table S1 in supplementary material.

## 186 **2.3 Soil incubation and As sequential extraction experiment**

187 Soil incubation experiments were designed to explore the effect of  $\alpha$ -MnO<sub>2</sub>  
188 nanorods on the variations of As fractionation in flooded paddy soil. To prepare the  
189  $\alpha$ -MnO<sub>2</sub> treated samples, 15 kg sieved soil was weighted carefully and packed into a  
190 polyethylene pot (50 cm×22 cm). Subsequently, the soil was amended with  $\alpha$ -MnO<sub>2</sub>  
191 nanorods to maintain the rates of 0.2%, 0.5%, 1.0% and 2.0% of soil weight. The pot  
192 was first pre-incubated for 24 h in the dark with soil moisture content being  
193 maintained at 70% field water holding capacity. After that, the pots were incubated at  
194 25°C in the growth chamber, with daily additions of ultra-pure water to maintain the  
195 water level of 3cm above the soil surface.

196 After 90 days, the soil samples were collected from the surface (0-20 cm depth)

197 of the soil profile. After being air-dried at ambient temperature, obtained soil will first  
198 ground to pass through 1mm screen, and then ground again using agate mortar and  
199 passed through 0.15 mm screen prior to analysis. A sequential As fractionation  
200 schemes was employed to determine the operationally defined As fractionation(Van et  
201 al., 2003; Wu et al., 2006). The detail operation procedure was described in  
202 supplementary material. (Table S2). All the treatments and extractions procedures  
203 were run in triplicates unless stated otherwise. The extraction efficiency of arsenic  
204 fractionation was presented in Table S3.

#### 205 **2.4 Pot experiment designs**

206 The pot experiment was carried out in a greenhouse of Hunan agricultural  
207 university. Firstly, 15.0 kg homogenized arsenic contaminated soil was packed in  
208 each polyethylene pot with a height of 50 cm and a diameter of 22 cm. Ammonium  
209 phosphate ( $(\text{NH}_4)_3\text{PO}_4 \cdot 3\text{H}_2\text{O}$ ), urea ( $\text{CO}(\text{NH}_2)_2$ ), potassium carbonate ( $\text{K}_2\text{CO}_3$ ), were  
210 added to each pot as basal fertilizers at dosage of 4.29, 2.93, and 3.30 g for N, P, and  
211 K supply, respectively. Then the soil was amended with  $\alpha$ - $\text{MnO}_2$  nanorods at rates of  
212 0.2%, 0.5%, 1.0% and 2.0% of soil weight. Each pot was then saturated with distilled  
213 water and drained down to an equilibrium state for 7 days under natural conditions.  
214 All the treatments were triplicated and randomly arrangement and three blank controls  
215 (without  $\alpha$ - $\text{MnO}_2$  nanorods addition) were provided.

216 The rice seeds (*O. sativa L* Yuzhenxiang, obtained from Hunan Rice Research  
217 Institute) were disinfected in 30%  $\text{H}_2\text{O}_2$  solution for 10 minutes, followed by thorough

218 washing with deionized water and soaking in deionized water for 24 h. Rice seeds  
219 were germinated in moist vermiculite trays until the three-leaf stage and then  
220 transplanted into pots. During the whole growth period, all pots were irrigated with  
221 distilled water daily to maintain the water level of 3 cm above the soil surface.  
222 Porewater samples were collected at a 15-days interval after tillering stage (after 45  
223 days) using a porous fiber tube. The pH, Mn and As concentrations in soil solutions  
224 were analyzed. Rice was harvested at the 105th day. At each growth stage (tillering,  
225 heading and maturing stages) rice plants were collected, digested, and then the  
226 concentrations of Mn and As in the organs (roots, stems, leaves, husk and grains) of  
227 rice plants were analyzed.

## 228 **2.5 Field application experiment designs**

### 229 **2.5.1 Experimental design**

230 The field experiment has carried out in May 2013 at a paddy field in Dengjatang,  
231 Chenzhou City, Hunan Province, (25°36'N, 113°00'E). The paddy fields were divided  
232 into 1.5 m ×1.5 m sub-plots with a 40-cm buffer zone between each. Before rice  
233 planting, the top soil (0–20cm depth) was subject to manual plowing.  $\alpha$ -MnO<sub>2</sub>  
234 nanorods was then added into the soil at a rate of 0.2%, 0.5%, 1.0% and 2.0% of soil  
235 weight (0-20 cm), respectively, and thoroughly mixed with top soil. All treatment was  
236 conducted in triplicate with a completely randomized factorial design, and three blank  
237 controls (without  $\alpha$ -MnO<sub>2</sub> nanorods addition) were provided. Each plot was then let to  
238 equilibrium for 7 days under natural conditions. Rice cultivars used in the pot

239 experiment (Yuzhenxiang) were also used in the field experiment. Rice seedlings  
240 were transplanted after germination for 30 days (on June 6, 2013) and harvested on  
241 September 30, 2013. To facilitate in situ sampling of pore water, during the growth of  
242 rice, ‘Rhizon’ soil solution samplers (Rhizon Research Products, Wageningen, The  
243 Netherlands) were buried in each plot while the rice was transplanted. During the  
244 whole growth period, water layer of about 3.0 cm above the topsoil of the paddy field  
245 was maintained. The other cultivation methods were the same as the local paddy  
246 cultivation methods until the rice has matured.

#### 247 **2.5.2 Sampling and, analyses**

248 Extractions of pore water were conducted in the tillering stage (45 days after  
249 germination) and were extracted every 15 days during the last period (days 45-105).  
250 The soil solution pH was recorded at the same time intervals as for pore water  
251 sampling. The concentrations of Mn in pore water were measured in acidified  
252 subsamples by inductively coupled Plasma optical emission spectrometer (ICP-OES,  
253 PerkinElmer Optima 8300, USA). As concentrations in soil pore water was  
254 determined by atomic fluorescence spectrometer (AFS-920, Beijing Titan Instruments  
255 Co., Ltd.). At each specifically growth period, the plants sample was collected at the  
256 tillering, heading and maturing stages. Rice plant samples were separated into roots,  
257 stems, leaves and grain. And washed three times using distilled water, the cleaned  
258 plant samples were placed in an oven at 105°C for 2 h and dried at 70°C for 3 days to  
259 constant weight, and then ground to pass a 100-mesh sieve with a micro plant

260 grinding machine.

261 The method for total As digestion and determination in rice plants was conducted  
262 following the protocol of GB/T 5009.11-2003 which issued by Ministry of  
263 Environmental Protection (MEP) of China (Geng et al., 2017). Typically, 1.0 g of dry  
264 rice sample was digested using a mixture of acids (4:1 HNO<sub>3</sub>: HClO<sub>4</sub>, v/v) at 180°C  
265 on a graphite digestion furnace. After digestion, the solution will let to cool down to  
266 ambient temperature and made to 25 mL using UP water, each digested solution will  
267 store in 50mL polyethylene bottle at 4°C before analysis. As concentrations in plants  
268 tissues will determined by atomic fluorescence spectrometer (AFS-920, Beijing Titan  
269 Instruments Co., Ltd.), Mn concentrations will measure by ICP-OES (Optima8300  
270 PerkinElmer). For quality assurance and quality control purposes, blanks and standard  
271 plant reference material (shrub branches and leaves GBW07603 (GSV-2), rice  
272 material (GBW10010 (GSB-1) were obtained from China Standard Materials  
273 Research Center, Beijing, P.R. China and digested along with the unknown samples  
274 and used for the QA/QC program. All the glassware was washed with detergent firstly,  
275 soaked with 20% HNO<sub>3</sub> solution for 24 h, and then rinsed with UP water for three  
276 times before use.

## 277 **2.6 Statistical analyses**

278 All statistical analyses were performed with SPSS 22.0 software (SPSS Inc.,  
279 Chicago, IL, USA). Differences between the control and treatment samples were  
280 determined using ANOVA and Tukey multiple comparisons analysis with  $p < 0.05$

281 indicating statistical significance. Correlations were obtained by Pearson correlation  
282 coefficient in bivariate correlations.

283

## 284 **3. Results**

### 285 **3.1 Characterization of synthesized $\alpha$ -MnO<sub>2</sub> nanorods**

286 The x-ray diffraction (XRD) pattern and scanning transmission electron  
287 microscopy (SEM) images of the synthesized  $\alpha$ -MnO<sub>2</sub> nanorods are shown in [Fig.S1](#),  
288 [Fig.S2](#), respectively. It can be seen that manganese dioxide is clustered; the structure  
289 is uniformly well dispersed spherical agglomerate particles. High-magnification SEM  
290 images showed that the  $\alpha$ -MnO<sub>2</sub> is an urchin-like spherical with a diameter of 1-1.5  
291  $\mu$ m, which consists of several straight and radially grown nanorods with uniform  
292 diameter around 30-40nm ([Fig.S2a, b](#)). The synthesized  $\alpha$ -MnO<sub>2</sub> nanorods has an  
293 obvious characteristic diffraction peak in the XRD pattern ([Fig.S1](#)), which indicated  
294 that the high crystallization degree of nanostructured manganese dioxide, and the  
295 characteristic peak was also in agreement with the standard data given in its JCPDS  
296 card (24-0072).

### 297 **3.2 Effects of different amount of $\alpha$ -MnO<sub>2</sub> nanorods on distribution of arsenic** 298 **fractionation**

299 The As sequential extraction procedure is widely used to evaluate As distribution  
300 within soil fractionation, which can help us to understand the mobility and

301 bioavailability of As in soil(Jin et al., 2011; Wenzel et al., 2001; Zhang et al.,  
302 2017).The effect of different dosages of  $\alpha$ -MnO<sub>2</sub> nanorods on the distribution and  
303 percentages of Arsenic fractionation in paddy soil are presented in Fig.1.

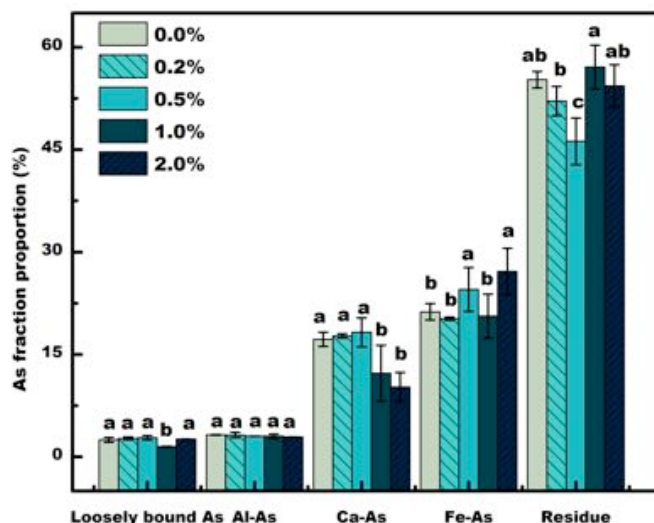
304 In general, the application of  $\alpha$ -MnO<sub>2</sub> amendment increased the residual  
305 fractionation and reduced the effective forms of As to some extent, indicating that  
306  $\alpha$ -MnO<sub>2</sub> can effectively control the bioavailability of As in soil. As shown in Fig.1, in  
307 the treated and untreated soil, loosely bound As comprised the smallest proportions of  
308 all the As fractionation (<3%); what's more, the content of loosely bound As in the  
309 soil with 1.0% MnO<sub>2</sub> treatment was significantly lower than that in other treatment.  
310 However, residual fractionation contained the most proportions of As (about 50%),  
311 whether or not to add  $\alpha$ -MnO<sub>2</sub> into soil. Besides, proportions of residual As in the  
312 1.0% MnO<sub>2</sub> treated soil was increased to 57.08% which indicated that the addition of  
313 1.0% MnO<sub>2</sub> increased the residual As and reduced the other forms of As in the soil.

314 For binding state-As (Al-As, Ca-As and Fe-As), there was no significant  
315 difference in the content of Al-As in the soil after treatment with different amounts of  
316  $\alpha$ -MnO<sub>2</sub>, whereas Ca-As decreased to 10.23% after treatment with 2%  $\alpha$ -MnO<sub>2</sub>; and  
317 with the increase of concentration, Ca-As content showed an obviously decreasing  
318 trend, which indicated that the addition of  $\alpha$ -MnO<sub>2</sub> in paddy soil has a certain  
319 inhibitory effect on the binding of As and Ca.

320

321





322 Fig.1. Fraction distributions of arsenic in paddy soil amended with different amounts of  $\alpha$ -MnO<sub>2</sub>; different  
 323 letters indicate significant difference between different treatments ( $P < 0.05$ ), arsenic fraction tested was  
 324 separately from each other.

325 For Fe-bound As, there was no regular change of Fe-As in the soil after the  
 326 addition of  $\alpha$ -MnO<sub>2</sub>. However, it can be seen that the content of Fe-As in soils  
 327 increased to 24.53% and 27.16% at rates of 0.5% and 2.0%, respectively. However, at  
 328 dosages of 0.2% and 1%, the amount of Fe-As in the soil has reduced, and the  
 329 addition of 1% was more obvious, which was 20.62%.

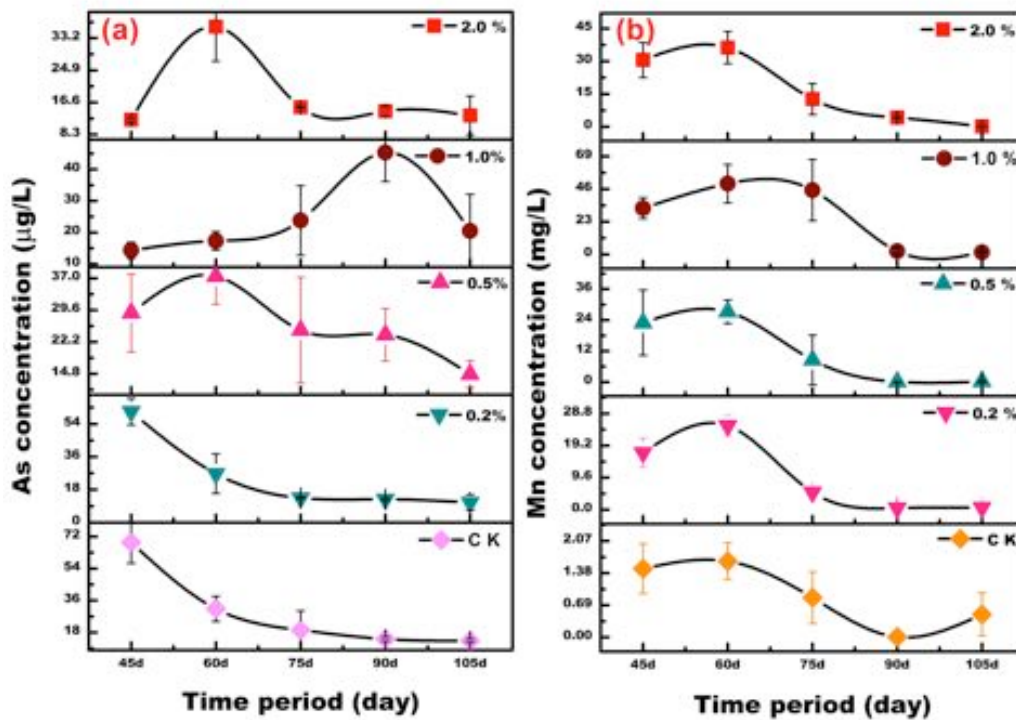
### 330 3.3 Pot experiments

#### 331 3.3.1 Effect of $\alpha$ -MnO<sub>2</sub> on the dynamic pH variations of soil solution

332 The dynamics variations of pH in the pore water during growth of rice under  
 333 treatments of different amounts of  $\alpha$ -MnO<sub>2</sub> were presented in Fig.S3. In general,  
 334 during the whole growth stage (45-105 days), the soil pore water pH either increased  
 335 to or remained stable in the near-neutral range after amended with different amounts  
 336 of  $\alpha$ -MnO<sub>2</sub>. The pH range of the soil solution was around 7.36-7.55 for the 45th day,  
 337 which was higher than the pH (7.25) of CK (Control treatments). The highest pH

338 value of the pore water was recorded at the 45th day (7.25-7.55). Afterwards, the pH  
 339 of the pore water decreased with the rice growth and reached the lowest value  
 340 (6.28-6.76) at the 105th days. Compared to the control,  $\alpha$ -MnO<sub>2</sub> treatments slightly  
 341 reduced the pH of the paddy soil under flooded condition, the pH was reduced by  
 342 0.58-1.06 unit after supplementation with  $\alpha$ -MnO<sub>2</sub>.

343 **3.3.2 Effect of  $\alpha$ -MnO<sub>2</sub> on the dynamic variations of As and Mn in pore water**



344 Fig.2. Dynamics variations of pore water As (a) and Mn (b) in the  $\alpha$ -MnO<sub>2</sub> treatments throughout the rice  
 345 cultivation period. Data are means SE (n= 3).

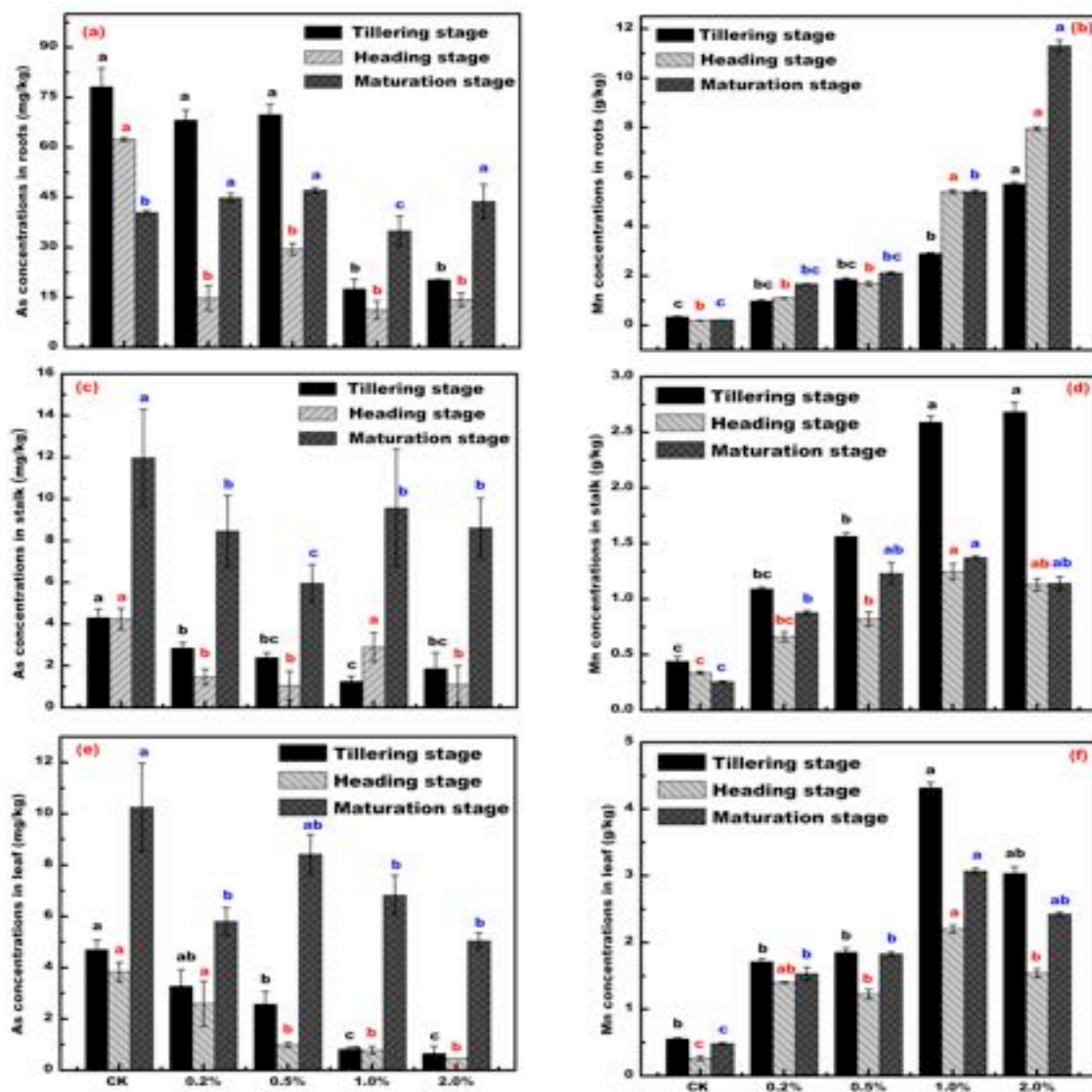
346 After treatments with different dosage of  $\alpha$ -MnO<sub>2</sub> the dynamic variation of  
 347 arsenic and manganese content in pore water at different growth period of rice is  
 348 shown in Fig.2. Different reduction patterns of arsenic in soil pore water were  
 349 observed among with different treatments. Regardless of the addition of  $\alpha$ -MnO<sub>2</sub>, the  
 350 arsenic content in soil pore water of CK was decreased from the 45th day to the 105th

351 day, and reaching the minimum value of  $13.26 \pm 0.94 \mu\text{g}\cdot\text{L}^{-1}$  at the 105th day; possibly  
352 due to the adsorbed by newly formed endogeneity amorphous iron oxides (Amstaetter  
353 et al., 2012; Cismasu et al., 2015). However, compared with CK, the content of  
354 arsenic in pore water after adding  $\alpha\text{-MnO}_2$  with different dosages decreased markedly  
355 at the 45th day. All treatments showed an obvious dosage dependent reduction trend  
356 of arsenic in soil pore water. Similarly, the decline trend was observed between CK  
357 and 0.2% treatments; however, with the increasing of dosages the content of arsenic  
358 began to rebound after 45 days. Arsenic concentrations peaked at 60 days of reaction  
359 at 0.5% treatments; 90 day for 1.0% treatments and 60 day of 2.0% treatments. In  
360 spite of fluctuation, what worth affirming was that arsenic in soil pore water still  
361 decreased to a constant level ( $10.94\text{-}14.69 \mu\text{g}\cdot\text{L}^{-1}$ ) at the end of rice cultivation period  
362 (90-105 day), except for 1% treatment, nearly 2-fold ( $20.49 \mu\text{g}\cdot\text{L}^{-1}$ ) increased in  
363 porewater As was observed during 90-105 day.

364 Unlike As,  $\alpha\text{-MnO}_2$  treatments increased porewater Mn levels (Fig.2b), four  
365 treatments (0.2%, 0.5% ,1.0% and 2.0%) showed that substantial increased in the  
366 porewater Mn concentration at the 45th day, whereas Mn concentration in the CK soil  
367 porewater remained low level throughout the whole cultivation period (45-105 days).  
368 What's more, Mn concentrations kept increasing after another 15 days; with 17-33  
369 folds augment compared with that of control soil. This is more likely coupled with the  
370 enhanced dissolution of manganese resulting from oxidation of As(III) to As(V) by  
371 manganese oxide (Xu et al., 2017; Z et al., 2017). Yet, effluent Mn(II) concentrations  
372 in soil porewater began to drop at the 60th day, with concentrations declining to a

373 constant level of 0.13-0.60 mg·L<sup>-1</sup> after 90 days of cultivation. Furthermore, among  
 374 all the four treatments, 1.0 % retained the highest porewater Mn dissolution rate  
 375 compared with other treatments during day 45-75 days and reaching a peak of 49.77  
 376 mg·L<sup>-1</sup> on the 60th day. In the meantime, however, the other three treatments have  
 377 already dropped to low levels (5.2-12.6 mg·L<sup>-1</sup>).

378 **3.3.3 Effect of  $\alpha$ -MnO<sub>2</sub> on the accumulation of As and Mn in rice plants parts**  
 379 **during different growth stage**



380 Fig.3. As and Mn concentrations in the root (a, b), straw (c, d), leaf (e, f) in the  $\alpha$ -MnO<sub>2</sub> treatments; Data are

381 means SE (n= 3), different letters indicate significant difference between different treatments ( $P < 0.05$ ),  
382 significant tests are separate from each other (black letter indicates tillering stage, red letter indicates  
383 heading stage, blue letter indicates maturation stage)

384 The contents of As and Mn in different parts of rice at various growth stages are  
385 shown in Fig.3. Three different rice growth stages (Tillering, heading and mature  
386 stage) were selected to estimate the efficiency of  $\alpha$ -MnO<sub>2</sub> in controlling the  
387 accumulation of As and Mn in rice. In general, regardless of the addition of  $\alpha$ -MnO<sub>2</sub>,  
388 the distribution pattern of arsenic in rice roots, stems and leaves follows the order of  
389 roots > stems > leaves. However, with the addition of  $\alpha$ -MnO<sub>2</sub>, the arsenic content in  
390 various parts of rice at each growth period was reduced to varying degrees compared  
391 with the CK. That is, the addition of  $\alpha$ -MnO<sub>2</sub> can effectively impede the migration of  
392 arsenic to rice plants. In  $\alpha$ -MnO<sub>2</sub> treatments, root As was decreased by 10.63-77.51%  
393 at tillering stage (Fig.3a), 52.71-81.94% at heading stage compared to the control.  
394 However, the interesting thing is that the reduction rate of arsenic in the mature stage  
395 was much lower than that of the other two growth period, which was indicated that  
396 the heading and tillering stage may be the key time period to control the transportation  
397 and migration of As (Li et al., 2015; Zheng et al., 2011).

398 On the contrary, the distribution pattern of Mn content in rice roots was clearly  
399 different from that of As in rice. Compared with CK, the Mn content in various parts  
400 of rice plants has significantly increased ( $p < 0.05$ ) at different growth stages after  
401 addition of  $\alpha$ -MnO<sub>2</sub> and the increasing trend was obviously dosage dependent, which  
402 illustrated that the order of Mn in roots, stems and leaves of rice was: 2.0% > 1.0% >  
403 0.5% > 0.2% > CK (Fig.3b). The overall Mn concentration in rice roots was increased  
404 by 1.9-15.87 times at tillering stage, 4.58-39.46 times at heading stage and 6.5-49.89

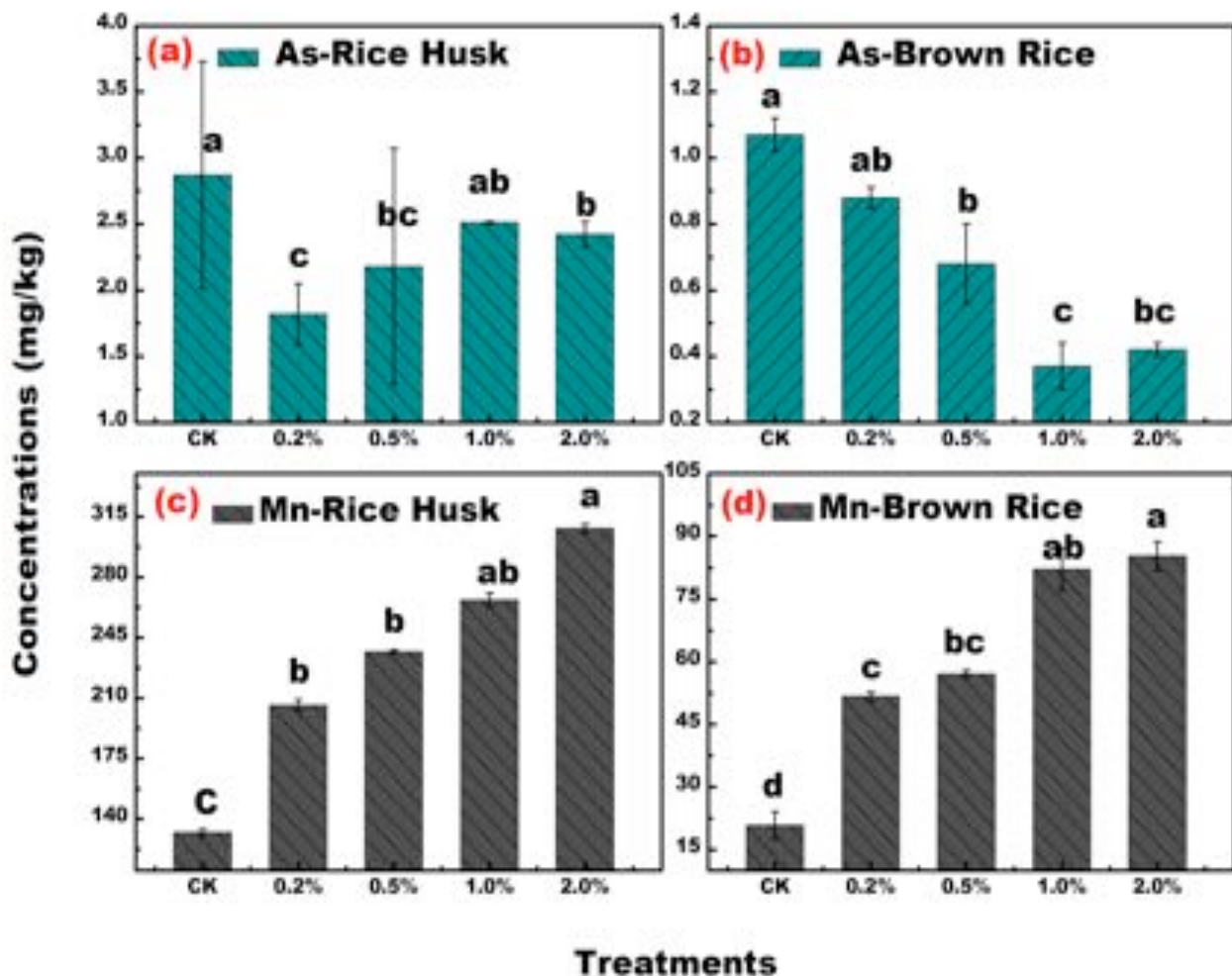
405 times at the mature stage, respectively.

406 Although  $\alpha$ -MnO<sub>2</sub> treatments were effective in reducing and accumulating of As  
407 and Mn in rice roots; their effects, however, on As, Mn transportation in the straw and  
408 leaf was less satisfactory. For the re-distribution of As in rice stalk and leaf, regardless  
409 of the addition of  $\alpha$ -MnO<sub>2</sub> and rice growth period sequences, the higher accumulation  
410 efficiency were observed at mature stage for both stalk and leaf; which indicated that  
411 mature stage were the crucial period for the translocation and migration of As in rice  
412 (Fig.3ce). However, the accumulation of Mn in stalks and leaves showed different  
413 patterns (Fig.3df), rice tended to accumulate more Mn during tillering stage, which  
414 was probably due to the enhanced dissolution of Mn in soil porewater at early stages  
415 (45-60 days) of rice growth after amended with  $\alpha$ -MnO<sub>2</sub> nanorods.

416 In addition, the observed results also implied that the re-distribution of As in rice part  
417 did not interfered by the added  $\alpha$ -MnO<sub>2</sub> after the tillering stage and this phenomenon  
418 was less time-dependent; which also confirmed that the As was sequestered in rice  
419 roots and thus the subsequent influx of As into other rice parts was restrained  
420 (Fig.3ce).

421 The content of As and Mn in brown rice and husk can further prove this  
422 phenomenon (Fig.4). The addition of  $\alpha$ -MnO<sub>2</sub> Nano-rods significantly reduced the  
423 total arsenic content in brown rice and husk ( $p < 0.05$ ), while the Mn content was  
424 significantly increased ( $p < 0.05$ ). Compared with CK, the contents of total arsenic in  
425 the husks decreased by 36.4%, 24.0%, 12.6% and 15.5%, respectively. Furthermore,  
426 the content of total arsenic in brown rice was decreased by 17.8%, 36.4%, 65.4% and

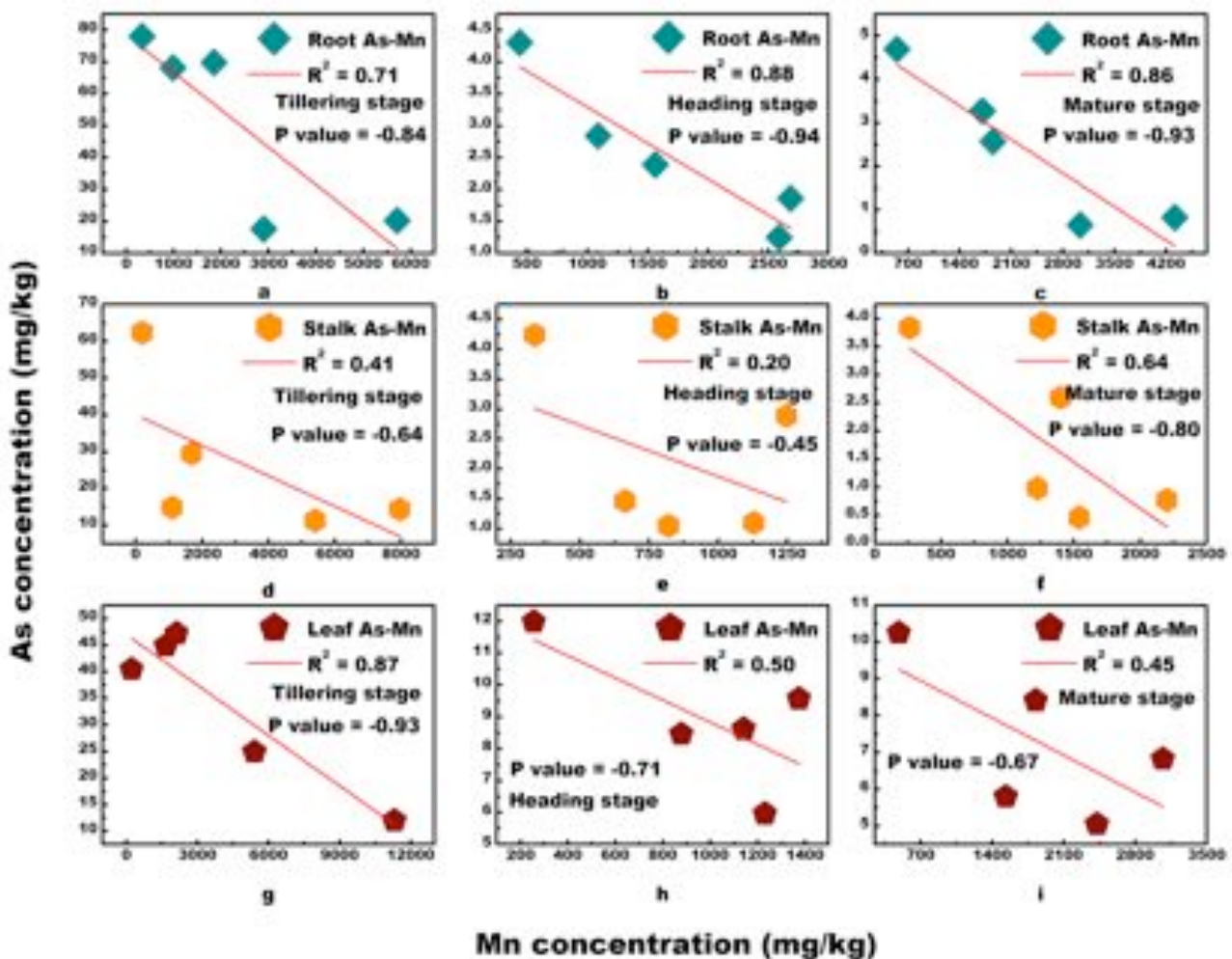
427 60.7%, respectively, which demonstrated that the addition of  $\alpha$ -MnO<sub>2</sub> nanorods can  
 428 effectively prevent arsenic uptake by brown rice. Meanwhile, Mn concentrations in  
 429 rice husk and brown rice increased in a dosage dependent way, which demonstrated  
 430 that the Mn concentrations increased with increasing dosages of  $\alpha$ -MnO<sub>2</sub> nanorods.  
 431 The content of Mn in the husk increased by 55.8%, 79.3%, 102.0% and 133.3%,  
 432 respectively; and the content of Mn in brown rice increased by 148.7%, 174.6%,  
 433 295.5% and 310.4%, respectively (Fig.4).



434 Fig.4 Concentrations of As and Mn in rice husk and brown rice (Pot experiment),(a) As-rice  
 435 husk, (b) As-brown rice,(c) Mn-rice husk,(d) Mn-brown rice; Data are means SE (n= 3),  
 436 different letters indicate significant difference between different treatments ( $P < 0.05$ ).

437 **3.3.4 Relationships between As and Mn concentration in rice plants parts under**  
 438 **different growth stages**

439 To further identify the relationship between the concentrations of As and Mn in  
 440 rice (Fig.S4) and different growth stages (Fig.5), we performed a correlation analysis;  
 441 and the results were presented in Fig.S4 and Fig.5 The concentration of As showed an  
 442 obviously significant negative correlation ( $p < 0.05$ ) with the amount of Mn in the rice,  
 443 indicating that the As content of rice plants decreased significantly with the increase  
 444 of Mn concentrations. And this also indicated that the application of  $\alpha$ -MnO<sub>2</sub>  
 445 nanorods was extremely effective at decreasing the available As in the soil



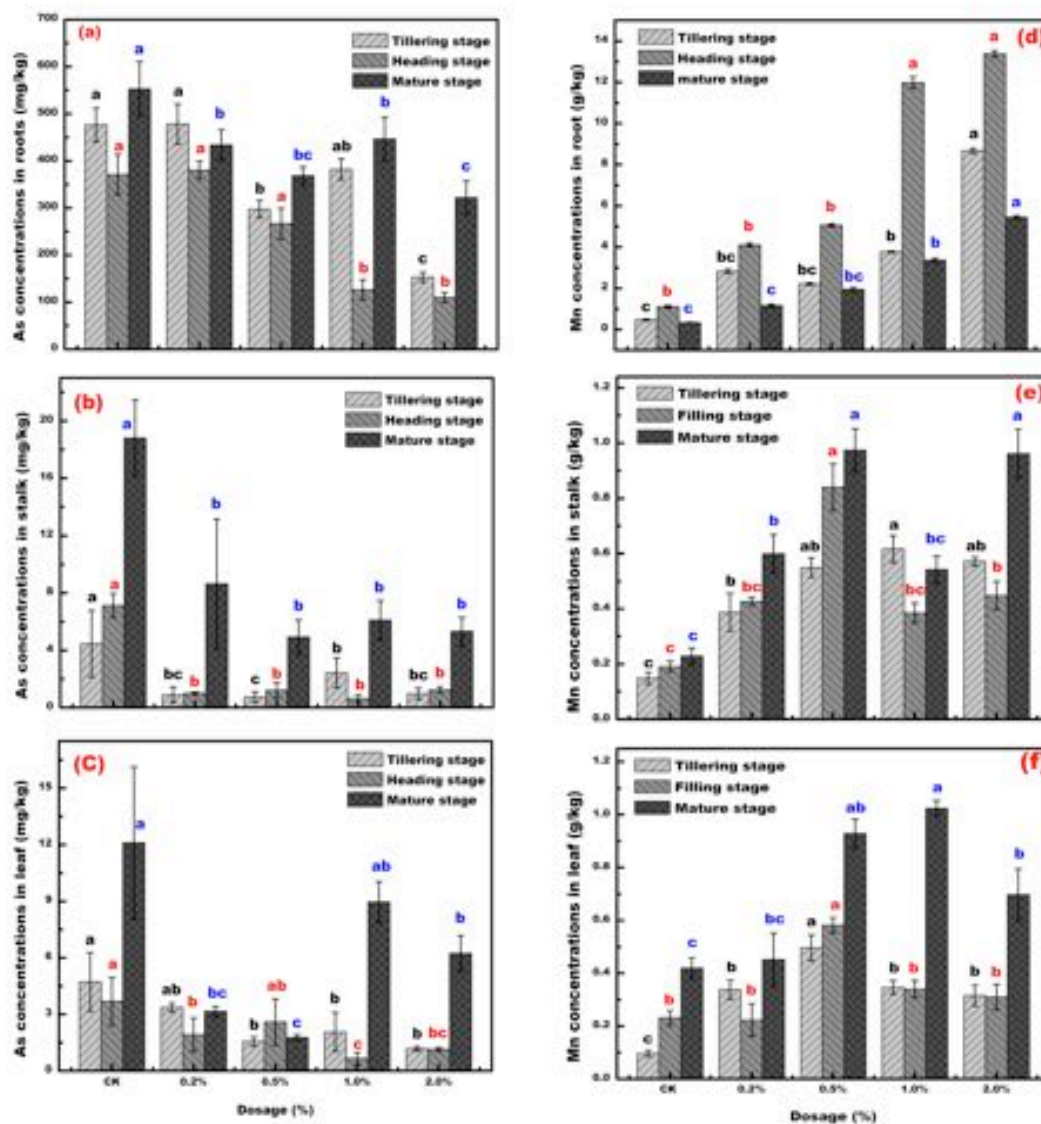
446 Fig.5. Relationships between As and Mn concentration in rice plants during different growth stage (a, b, c,



447 root-As-Mn), (d, e, f, stalk -As-Mn) and (g, h, I, leaf-As-Mn); Data are means SE (n= 3).

448 In the meantime, the relationships between As and Mn in different rice parts at  
449 different growth stages were also analyzed, and the correlations were presented in  
450 Fig.5, as can be seen from the above picture, overall As and Mn correlations in  
451 various parts showed obviously negative correlations. Especially for root As and Mn,  
452 their correlation showed higher  $R^2$  value compared with other two parts, regardless of  
453 the growth stages ( $R^2=0.71-0.88$ ,  $p<0.05$ ; Fig.5abc). In contrast, although at certain  
454 growth stages, the As and Mn in rice parts showed extremely high significance; their  
455 overall relationships in stalks ( $R^2=0.20-0.63$ ; Fig.5def) and leaves ( $R^2=0.44-0.87$ ;  
456 Fig.5ghi), however, were poor than roots As-Mn.

### 457 3.4 Field applications



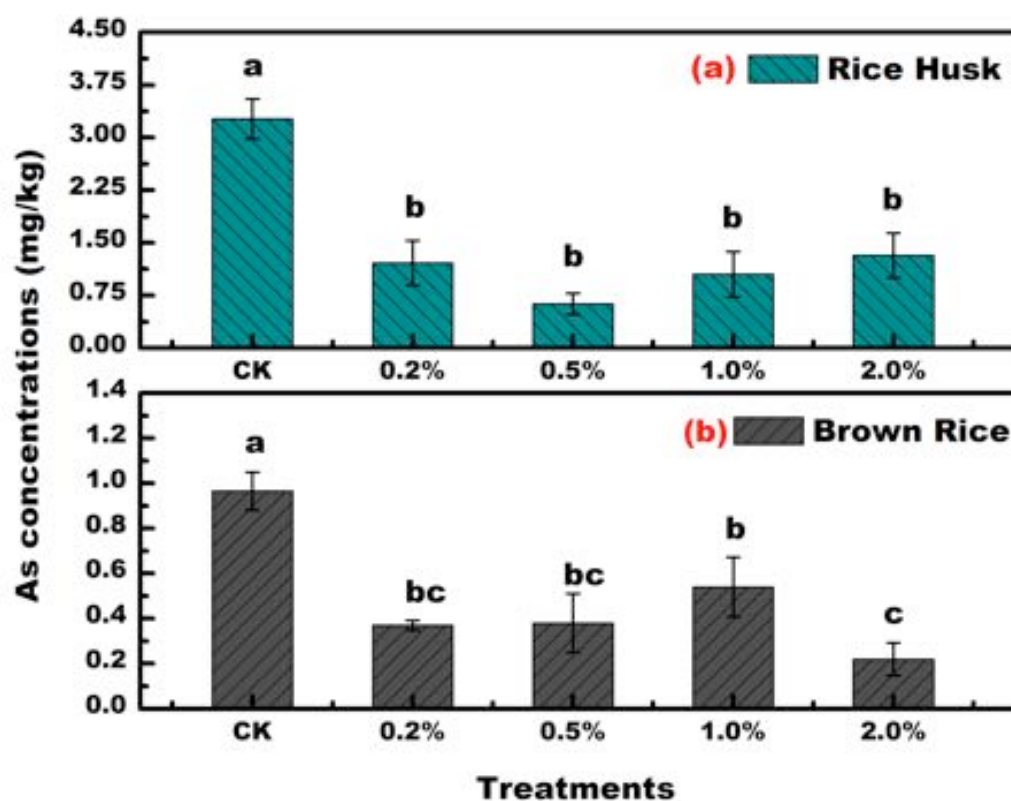
458

459 **Fig.6. As and Mn concentrations in the root (a, d), straw (b, e), and leaf (c, f) of rice in the  $\alpha$ -MnO<sub>2</sub>**  
 460 **treatments (Field application); Data are means SE (n= 3), different letters indicate significant difference**  
 461 **between different treatments ( $P < 0.05$ ), significant tests are separate from each other (black letter indicates**  
 462 **tillering stage, red letter indicates heading stage, blue letter indicates maturation stage)**

463 Previous studies have shown that the addition of  $\alpha$ -MnO<sub>2</sub> nanorods in  
 464 arsenic-contaminated soil can effectively control the transport of arsenic from soil to  
 465 rice in pot experiments. This result provides a theoretical basis for the application of  
 466  $\alpha$ -MnO<sub>2</sub> nanorods in field trials. With this in mind, field trials were designed to

467 further evaluate the effectiveness of  $\alpha$ -MnO<sub>2</sub> nanorods in controlling the mobility and  
468 bio-availability of arsenic in soil-rice interfaces under complex natural systems. The  
469 content of arsenic and manganese in different parts of rice at various stages in the  
470 field experiment was shown in Fig.6. With the addition of  $\alpha$ -MnO<sub>2</sub> nanorods, the  
471 arsenic content in various parts of rice at each period was reduced to varying degrees  
472 compared with the CK group (Fig.6b). It was also can be seen that the arsenic  
473 concentration in rice roots was much higher than that in the stalks and leaves.  
474 Furthermore, the similar results have been observed in stalks and leaves compared  
475 with pot experiment, in which rice tended to accumulate more As at mature stage.  
476 And the observed results also indicated that most of the As was sequestered in rice  
477 roots (Fig.6bc). Meanwhile, after treatments with different amounts of  $\alpha$ -MnO<sub>2</sub>  
478 nanorods, the content of Mn in various parts of rice plants increased significantly

479 ( $p < 0.05$ ) at different growth periods compared with the CK. And this result was  
 480 consistent with the results obtained in the pot experiment, which also proved that the  
 481  $\alpha$ -MnO<sub>2</sub> nanorods can indeed reduce the bio-availability of arsenic in soil. After  
 482 treatment with  $\alpha$ -MnO<sub>2</sub> nanorods, total As content in brown rice and husk was  
 483 significantly reduced (Fig.7;  $p < 0.05$ ). Arsenic content in the husk of CK was  
 484  $3.06 \pm 0.41 \text{ mg} \cdot \text{kg}^{-1}$  and  $0.96 \pm 0.08 \text{ mg} \cdot \text{kg}^{-1}$  in brown rice. Compared with CK, the  
 485 contents of total As in husks decreased by 60.5%, 79.6%, 65.7%, and 56.9%,  
 486 respectively; and the content of total As in brown rice was decreased by 61.5%,  
 487 60.4%, 43.4%, and 77.1%, respectively. Among them, the lowest content



488 ( $0.22 \text{ mg} \cdot \text{kg}^{-1}$ ) of As in brown rice was obtained under the condition of 2.0%  
 489 treatments.

490 Fig.7. Concentrations of As in rice husk and brown rice (Field application), (a) rice husk, (b) brown rice;  
 491 Data are means SE ( $n = 3$ ), different letters indicate significant difference between different treatments ( $P <$   
 492  $0.05$ ).

## 493 **4. Discussion**

### 494 **4.1 Effects of different dosages of $\alpha$ -MnO<sub>2</sub> nanorods on the solid-liquid** 495 **partitioning of As in paddy soil**

496 Since long is it established that the toxicity, activity and bioavailability of As in  
497 paddy soil are closely related to its presence in the soil (Yamaguchi et al., 2011). The  
498 hazards of As in soil are not only related to its content, but also related to its  
499 effectiveness in the soil and its associated binding forms (classification). In the  
500 present study, a 90d soil incubation experiment combined with sequential extraction  
501 procedure, therefore, was conducted to study the arsenic fractionation transformed in  
502 soil under flooded conditions after amended with  $\alpha$ -MnO<sub>2</sub> nanorods; because it can  
503 furnish us an indication for the mobility and bioavailability of As in paddy soil after  
504 amended with  $\alpha$ -MnO<sub>2</sub> nanorods. As can be draw from the above results (Fig.1), after  
505 treatment with different amounts of  $\alpha$ -MnO<sub>2</sub> nanorods the content of effective As  
506 decreased with the increasing of residual As and insoluble binding As (Ca-As and  
507 Fe-As), indicating that supplementation of  $\alpha$ -MnO<sub>2</sub> nanorods can effectively control  
508 the bio-availability of As in soil and reduced the associated influx of As into rice  
509 plants. Generally, loosely bound As (water soluble and exchangeable As) are highly  
510 bio-availability, and they are easily absorbed by organisms, resulting in greater  
511 toxicity. The Fe-As and other encapsulated state As are not easily absorbed by  
512 organisms and enter the water body, their harmfulness is relatively low. Fe-As, Al-As  
513 bind closely to soil, their toxicity to organisms are generally less than Ca-As.

514 (Herreweghe et al., 2003) found that water-soluble As and exchangeable As are  
515 soluble As in the soil or As adsorbed on the surface of soil particles, which accounts  
516 for less than 3% of total As. Similar results have been observed in our experiment, the  
517 proportion of loosely bound As in the soil was less than 3% regardless of the addition  
518 of  $\alpha$ -MnO<sub>2</sub> nanorods, which indicated that the mobilization pool of As in paddy soil  
519 depends on other forms. Thus, the content of binding As (such as Fe-As, Al-As) may  
520 be the most contributing component in soil. Under aerobic conditions, As(V) is  
521 strongly adsorbed on most mineral constituents, including Fe and Al(hydr)oxides  
522 (Goldberg, 2002) whereas, arsenite is more mobile because of its poor affinity for  
523 mineral surfaces (Han et al., 2011). Manganese oxide has long been regarded as natural  
524 occurring powerful oxidants (Han et al., 2011; Ren et al., 2013), which can rapidly  
525 convert As(III) to As(V) over the pH range of 4~8.2 under natural conditions (Bruce  
526 A. Manning et al., 2002). In the present study, in order to simulate an authentic rice  
527 growing environment, the soil has been flooded with water along with the whole  
528 incubation period. It is well accepted that incubation under flooded conditions can  
529 cause solid As to be distributed to liquid phase (Lemonte et al., 2017; Xu et al., 2017),  
530 in which the dominating As species was arsenite; so As can be re-mobilized into soil  
531 when As(V) is reduced to As(III). In spite of this circumstance, as can be seen from  
532 the Fig.1, the content of Fe-As still increased after treatment with 0.5% and 2.0% of  
533  $\alpha$ -MnO<sub>2</sub> nanorods, which proved that the increased binding state As was more likely  
534 due to the oxidation of As(III) into As(V) by  $\alpha$ -MnO<sub>2</sub> nanorods and subsequently  
535 resulted to the enhanced adsorption onto ferric(hydr)oxides and Al mineral. The

536 subsequently re-allocation of As into the soil solution was, thus effectively reduced.  
537 Besides, the content of Ca-As was decreased with an increase in the associated  
538 residual As at the dosage of 1%, which indicated that the other encapsulated As  
539 fractionation was also transformed to less effective forms.

540 Combined the obtained results in soil incubation experiments, which can  
541 provide us with a reliable theoretical basis for our subsequent experiment. The  
542 hypothesis of the present study was proposed that in the rice rhizosphere  
543 micro-environment, addition of  $\alpha$ -MnO<sub>2</sub> nanorods can affect the chemical speciation  
544 of As in the soil solution through in situ oxidation which in turn affect the  
545 bio-availability and mobility of As for rice uptake. As already discussed in soil  
546 incubation experiment, the partitioning of As into the soil solution was significantly  
547 controlled by As fractionation transformed. This part of observed results can be  
548 further proved by the dynamic monitoring of As variations in soil solution (Fig.2ab).  
549 As can be seen from Fig.2a, the content of porewater As was significantly decreased  
550 as a dosage dependent way at the 45th day with the increasing content of  $\alpha$ -MnO<sub>2</sub>  
551 nanorods. And during the whole growth stages (45-105 days), in spite of slightly  
552 fluctuation, the overall concentrations of As was decreased. Several studies have been  
553 deciphered that the effluent of Mn is attributed to the process of arsenite oxidation by  
554 manganese oxides (Lafferty et al., 2010; Oscarson et al., 1983; Tournassat et al.,  
555 2002); and it is widely accepted that the oxidation of As(III) to As(V) involves in a  
556 two-step process, including the release of Mn(II) and sorption of Mn(II) on oxidation  
557 intermediate (Nesbitt et al., 1998).

558 Our results are extremely consistent with those previous studies. As can be  
559 drawn from the above picture (Fig.2b) the content of Mn has been increased to an  
560 extraordinary magnitude (17-33 folds) compared with the untreated soil. Nevertheless,  
561 unfortunately the persistence increasing of Fe(II) and Mn(II) in soil porewater under  
562 reduced conditions at early growth stages (45-60 days) can inhibited the abiotic  
563 oxidation of As(III) by  $\alpha$ -MnO<sub>2</sub> nanorods (Ehlert et al., 2014). Another study reported  
564 by Chen et al. (2006) showed that the oxidation rates could be also impaired by soil  
565 organic matter(Chen et al., 2006). Those reported studies explained that why the Mn  
566 concentrations in the soil porewater tend to decrease with the rice growth time  
567 prolonged (60-105days) (Fig.2b).

#### 568 **4.2 Enhanced impeded of As accumulation in rice by $\alpha$ -MnO<sub>2</sub> nanorods.**

569 Combined the results which obtained from soil incubation experiments, we can  
570 draw a conclusion that the partitioning of As into soil porewater has been rigorous  
571 hindered (Fig.2a). Moreover, the impeded As elution has also in turn affected the  
572 accumulation of As into rice. But the interplay between the addition of  $\alpha$ -MnO<sub>2</sub>  
573 nanorods and As in plant cultivation systems was far more complexity than the pure  
574 soil incubation. Pot and field rice cultivation together with soil incubation  
575 experiments were therefore combined to clarify the effects of different amounts of  
576  $\alpha$ -MnO<sub>2</sub> nanorods on the accumulation and translocation of As into rice (Fig.3-7). On  
577 the basis of the present study, we believe that there are at least two factors appear to  
578 play crucial roles in controlling the As influx into rice plants.



579 Firstly, in situ oxidation of As(III) to As(V) in the presence of  $\alpha$ -MnO<sub>2</sub> nanorods  
580 leads to the subsequently enhanced adsorption of As onto endogenous iron(oxyhydr)  
581 oxides; greatly reduced the re-allocation of As into soil porewater, and thus directly  
582 cut down the total As transportation into rice parts. As can be seen from the above  
583 picture (Fig.3 and Fig.6) The addition of Mn oxides significantly impeded the  
584 accumulation of As into subterranean parts (roots  $p<0.05$ ); and the associated influx  
585 of As into aerial parts (stems, leaves, husk and brown rice) has been also obstructed  
586 (Fig.3 and Fig.6;  $p<0.05$ ). Correlations analysis (Fig.S4 and Fig.5) between As and  
587 Mn in rice parts can also prove that the transportation of As has been greatly limited.

588 Secondly, apart from those existing fact, As bioavailability could be also  
589 mediated through iron and manganese plaque formation on the rice roots and so  
590 influence As uptake by rice plants (Liu, 2005; Liu et al., 2005). Therefore, enhanced  
591 sequestrate of As by rice roots were probably due to the iron and manganese plaque  
592 formation of the rice roots (Fig.3a and Fig.5a). Besides, the addition of manganese  
593 oxides can also promote Fe(II) oxidation (Postma and Appelo, 2000); Ehlert et al.  
594 (Ehlert et al., 2014) reported that birnessite additions can promote Fe(II) oxidation to  
595 Fe(III), thereby creating newly-formed Fe(III) hydroxides which could serve as  
596 efficient sorbents for As(III).

597 Hence, by combination of the obtained facts, we can draw a conclusion that the  
598 addition of  $\alpha$ -MnO<sub>2</sub> nanorods served as a multifunctional role on the As mobilization  
599 and transportation in paddy fields. Firstly, the effects on the As fractionation in paddy  
600 soil leads to the less dissolution of As in soil porewater. Secondly, As(III) oxidation

601 triggered by  $\alpha$ -MnO<sub>2</sub> nanorods resulted to the adsorption of water soluble As(V) onto  
602 iron oxides. Lastly, the enhanced dissolution of Mn(II) and Fe(III) can lead to the  
603 more iron and manganese plaque formation, which can sequester more As on the  
604 surface of rice roots.

## 605 **5 Conclusions**

606 In the present study, soil incubation experiments which combined with pot and  
607 field rice cultivation trials were designed to evaluate the effectiveness of exogenous  
608  $\alpha$ -MnO<sub>2</sub> nanorods on the mobilization and transportation of As in soil-rice systems.  
609 Our results proved that the addition of  $\alpha$ -MnO<sub>2</sub> nanorods can effectively control the  
610 soil-to-solution partitioning of As under anaerobic conditions. The As fractionation  
611 can be transformed from effective forms into less effective forms impeded the  
612 re-allocation of As into soil porewater, and thus reduced the total amounts of As  
613 influx into rice. Besides, the enhanced oxidation of As(III) into As(V) by  $\alpha$ -MnO<sub>2</sub>  
614 nanorods greatly increased the adsorption of As onto indigenous iron(hydr) oxides,  
615 thus, reduced the soil porewater As. Furthermore, with the simultaneous  
616 co-occurrences of the oxidation intermediates of Mn(II) and Fe(III), which can  
617 probably lead to the enhanced formation of iron and manganese plaque on the surface  
618 of rice roots. Combined, the influx of As into aerial parts of rice plants (stems, husk  
619 and leaves) was strictly prohibited by rice roots. Nevertheless, it should be noted that  
620 the abiotic oxidation of As by  $\alpha$ -MnO<sub>2</sub> nanorods are greatly impaired by various  
621 environmental factors (such as DOM, microbial activities and ligands), thus, further

622 work is still needed to verify these results under fields or laboratory scales.

## 623 **Acknowledgement**

624 The authors are grateful for financial support from the National Science Foundation of  
625 China (41671475/21007014). The author feels extremely thankful to the anonymous  
626 reviewers, that work in this paper, for their respected comments and recommendations  
627 to increase the quality of this work.

628

## 629 **References**

- 630 Amstaetter K, Borch T, Kappler A. Influence of humic acid imposed changes of  
631 ferrihydrite aggregation on microbial Fe(III) reduction. *Geochimica Et*  
632 *Cosmochimica Acta* 2012; 85: 326-341.
- 633 BA M, SE F, B B, DL S. Arsenic(III) oxidation and arsenic(V) adsorption reactions  
634 on synthetic birnessite. *Environmental Science & Technology* 2002; 36: 976-81.
- 635 Balasubramanian N, Kojima T, Srinivasakannan C. Arsenic removal through  
636 electrocoagulation: kinetic and statistical modeling. *Chemical Engineering*  
637 *Journal* 2009; 155: 76-82.
- 638 Beiyuan J, Li JS, Dcw T, Wang L, Poon CS, Li XD, et al. Fate of arsenic before and  
639 after chemical-enhanced washing of an arsenic-containing soil in Hong Kong.  
640 *Science of the Total Environment* 2017; 599-600: 679-688.
- 641 Bontempi E. A new approach for evaluating the sustainability of raw materials  
642 substitution based on embodied energy and the CO<sub>2</sub> footprint. *Journal of*  
643 *Cleaner Production* 2017; 162.
- 644 Bruce A. Manning, ‡ SEF, Benjamin Bostick A, Suarez§ DL. Arsenic(III) Oxidation  
645 and Arsenic(V) Adsorption Reactions on Synthetic Birnessite. *Environmental*  
646 *Science & Technology* 2002; 36: 976.
- 647 Chen Z, Kim KW, Zhu YG, McLaren R, Liu F, He JZ. Adsorption (As<sup>III</sup>,V) and  
648 oxidation (As<sup>III</sup>) of arsenic by pedogenic Fe–Mn nodules. *Geoderma* 2006; 136:  
649 566-572.
- 650 Cismasu AC, Williams KH, Nico PS. Iron and carbon dynamics during aging and  
651 reductive transformation of biogenic ferrihydrite. *Environmental Science &*  
652 *Technology* 2015; 50.

653 Ehlert K, Mikutta C, Kretzschmar R. Impact of birnessite on arsenic and iron  
654 speciation during microbial reduction of arsenic-bearing ferrihydrite.  
655 *Environmental Science & Technology* 2014; 48: 11320-11329.

656 Fendorf S, Kocar BD. Biogeochemical processes controlling the fate and transport of  
657 arsenic: implications for South and Southeast Asia. *Advances in Agronomy*  
658 2009; 104: 137-164.

659 Fu QL, Liu C, Achal V, Wang YJ, Zhou DM. Aromatic Arsenical Additives (AAAs)  
660 in the Soil Environment: Detection, Environmental Behaviors, Toxicities, and  
661 Remediation. Vol 140, 2016.

662 Geng A, Wang X, Wu L, Wang F, Chen Y, Yang H, et al. Arsenic accumulation and  
663 speciation in rice grown in arsenic acid-elevated paddy soil. *Ecotoxicology &*  
664 *Environmental Safety* 2017; 137: 172.

665 Gil-Díaz M, Alonso J, Rodríguez-Valdés E, Gallego JR, Lobo MC. Comparing  
666 different commercial zero valent iron nanoparticles to immobilize As and Hg in  
667 brownfield soil. *Science of the Total Environment* 2017; 584-585.

668 Gil-Díaz M, Diez-Pascual S, González A, Alonso J, Rodríguez-Valdés E, Gallego JR,  
669 et al. A nanoremediation strategy for the recovery of an As-polluted soil.  
670 *Chemosphere* 2016; 149: 137-145.

671 Gilloaiza J, White SA, Root RA, Solísdominguez FA, Hammond CM, Chorover J, et  
672 al. Phytostabilization of Mine Tailings Using Compost-Assisted Direct Planting:  
673 Translating Greenhouse Results to the Field. *Science of the Total Environment*  
674 2016; 565: 451.

675 Goldberg S. Competitive Adsorption of Arsenate and Arsenite on Oxides and Clay  
676 Minerals. *Soil Science Society of America Journal* 2002; 66: 413-421.

677 Han X, Li YL, Gu JD. Oxidation of As(III) by MnO<sub>2</sub> in the absence and presence of  
678 Fe(II) under acidic conditions. *Geochimica Et Cosmochimica Acta* 2011; 75:  
679 368-379.

680 Herreweghe SV, Swennen R, Vandecasteele C, Cappuyns V. Solid phase speciation  
681 of arsenic by sequential extraction in standard reference materials and  
682 industrially contaminated soil samples. *Environmental Pollution* 2003; 122:  
683 323-342.

684 Jankong P, Visoottiviseth P, Khokiattiwong S. Enhanced phytoremediation of arsenic  
685 contaminated land. *Chemosphere* 2007; 68: 1906-1912.

686 Jin HP, Choppala GK, Bolan NS, Chung JW, Chuasavathi T. Biochar reduces the  
687 bioavailability and phytotoxicity of heavy metals. *Plant & Soil* 2011; 348: 439.

688 Kumpiene J, Lagerkvist A, Maurice C. Stabilization of As, Cr, Cu, Pb and Zn in soil  
689 using amendments--a review. *Waste Management* 2008; 28: 215.

690 Lafferty BJ, Gindervogel M, Sparks DL. Arsenite Oxidation by a Poorly Crystalline  
691 Manganese-Oxide 1. Stirred-Flow Experiments. *Environmental Science &*  
692 *Technology* 2010; 44: 8460-6.

693 Lei M, Tie B, Zeng M, Qing P, Song Z, Williams PN, et al. An arsenic-contaminated  
694 field trial to assess the uptake and translocation of arsenic by genotypes of rice.  
695 *Environ Geochem Health* 2013; 35: 379-390.

696 Lei M, Tie BQ, Song ZG, Liao BH, Lepo JE, Huang YZ. Heavy metal pollution and

697 potential health risk assessment of white rice around mine areas in Hunan  
698 Province, China. *Food Security* 2015; 7: 45-54.

699 Lemonte JJ, Stuckey JW, Sanchez JZ, Tappero RV, Rinklebe J, Sparks DL. Sea level  
700 rise induced arsenic release from historically contaminated coastal soils.  
701 *Environmental Science & Technology* 2017; 51.

702 Li B, Peng L, Wei D, Lei M, Liu B, Lin Y, et al. Enhanced flocculation and  
703 sedimentation of trace cadmium from irrigation water using phosphoric fertilizer.  
704 *Science of the Total Environment* 2017; 601-602: 485.

705 Li JS, Wang L, Cui JL, Poon CS, Beiyuan J, Dew T, et al. Effects of low-alkalinity  
706 binders on stabilization/solidification of geogenic As-containing soils:  
707 Spectroscopic investigation and leaching tests. *Science of the Total Environment*  
708 2018; 631-632: 1486.

709 Li M, Wang L, Jia Y, Yang Z. Arsenic speciation in locally grown rice grains from  
710 Hunan Province, China: Spatial distribution and potential health risk. *Science of*  
711 *the Total Environment* 2016; s 557–558: 438-444.

712 Li R, Zhou Z, Zhang Y, Xie X, Li Y, Shen X. Uptake and Accumulation  
713 Characteristics of Arsenic and Iron Plaque in Rice at Different Growth Stages.  
714 *Communications in Soil Science & Plant Analysis* 2015; 46: 2509-2522.

715 Liao X, Chen T, Xie H, Xiao X. Effect of application of P fertilizer on efficiency of  
716 As removal from As-contaminated soil using phytoremediation: Field study.  
717 *Acta Scientiae Circumstantiae* 2004.

718 Liao XY, Chen TB, Xie H, Liu YR. Soil As contamination and its risk assessment in  
719 areas near the industrial districts of Chenzhou City, Southern China.  
720 *Environment International* 2005; 31: 791-798.

721 Limmer MA, Wise P, Dykes GE, Seyfferth AL. Silicon Decreases Dimethylarsinic  
722 Acid Concentration in Rice Grain and Mitigates Straighthead Disorder.  
723 *Environmental Science & Technology* 2018; 52: 4809-4816.

724 Lin L, Gao M, Qiu W, Wang D, Huang Q, Song Z. Reduced arsenic accumulation in  
725 indica rice (*Oryza sativa* L.) cultivar with ferromanganese oxide impregnated  
726 biochar composites amendments. *Environmental Pollution* 2017; 231: 479.

727 Liu C, Yu HY, Liu C, Li F, Xu X, Wang Q. Arsenic availability in rice from a mining  
728 area: is amorphous iron oxide-bound arsenic a source or sink? *Environmental*  
729 *Pollution* 2015; 199: 95-101.

730 Liu L, Li W, Song W, Guo M. Remediation techniques for heavy metal-contaminated  
731 soils: Principles and applicability. *Science of the Total Environment* 2018; 633:  
732 206-219.

733 Liu R, Zhao D. Reducing leachability and bioaccessibility of lead in soils using a new  
734 class of stabilized iron phosphate nanoparticles. *Water Research* 2007; 41:  
735 2491-2502.

736 Liu WJ. Direct evidence showing the effect of root surface iron plaque on arsenite and  
737 arsenate uptake into rice (*Oryza sativa*) roots. *New Phytologist* 2005; 165: 91-97.

738 Liu WJ, Zhu YG, Smith FA. Effects of Iron and Manganese Plaques on Arsenic  
739 Uptake by Rice Seedlings (*Oryza sativa* L.) Grown in Solution Culture Supplied  
740 with Arsenate and Arsenite. *Plant & Soil* 2005; 277: 127-138.

741 Liu Z, Zhu QQ, Tang LH. Microelements in the main soils of China. *Soil Science*  
742 1983; 135: 40-46.

743 Ma JF, Yamaji N, Mitani N, Xu XY, Su YH, Mcgrath SP, et al. Transporters of  
744 Arsenite in Rice and Their Role in Arsenic Accumulation in Rice Grain.  
745 *Proceedings of the National Academy of Sciences of the United States of*  
746 *America* 2008; 105: 9931-9935.

747 Meharg AA. Arsenic in rice--understanding a new disaster for South-East Asia.  
748 *Trends in Plant Science* 2004; 9: 415-417.

749 Meharg AA, Jardine L. Arsenite transport into paddy rice ( *Oryza sativa* ) roots. *New*  
750 *Phytologist* 2003; 157: 39-44.

751 Nesbitt HW, Canning GW, Bancroft GM. XPS study of reductive dissolution of  
752  $\text{Fe}(\text{OH})_3$ -birnessite by  $\text{H}_3\text{AsO}_3$ , with constraints on reaction mechanism - Part 1.  
753 EXAFS studies of the geometry of coprecipitated and adsorbed arsenate.  
754 *Geochimica Et Cosmochimica Acta* 1998: 2097-2110.

755 Ohtsuka T, Yamaguchi N, Makino T, Sakurai K, Kimura K, Kudo K, et al. Arsenic  
756 dissolution from Japanese paddy soil by a dissimilatory arsenate-reducing  
757 bacterium *Geobacter* sp. OR-1. *Environmental Science & Technology* 2013; 47:  
758 6263-6271.

759 Okkenhaug G, Zhu YG, He J, Li X, Luo L, Mulder J. Antimony (Sb) and arsenic (As)  
760 in Sb mining impacted paddy soil from Xikuangshan, China: differences in  
761 mechanisms controlling soil sequestration and uptake in rice. *Environmental*  
762 *Science & Technology* 2012; 46: 3155.

763 Oscarson DW, Huang PM, Liaw WK, Hammer UT. Kinetics of Oxidation of Arsenite  
764 by Various Manganese Dioxides. *Soil Sci.soc.am.j* 1983; 47: 644-648.

765 Postma D, Appelo CAJ. Reduction of Mn-oxides by ferrous iron in a flow system:  
766 column experiment and reactive transport modeling. *Geochimica Et*  
767 *Cosmochimica Acta* 2000; 64: 1237-1247.

768 Ren HT, Jia SY, Wu SH, Liu Y, Hua C, Han X. Abiotic oxidation of Mn(II) induced  
769 oxidation and mobilization of As(III) in the presence of magnetite and hematite.  
770 *Journal of Hazardous Materials* 2013; s 254–255: 89-97.

771 Scott MJ, Morgan JJ. Reactions at Oxide Surfaces. 1. Oxidation of As(III) by  
772 Synthetic Birnessite. *Environmental Science & Technology* 1995; 29: 1898.

773 Seyfferth AL, Limmer MA, Dykes GE. On the Use of Silicon as an Agronomic  
774 Mitigation Strategy to Decrease Arsenic Uptake by Rice. *Advances in*  
775 *Agronomy* 2018.

776 Suda A, Makino T. Functional effects of manganese and iron oxides on the dynamics  
777 of trace elements in soils with a special focus on arsenic and cadmium: A review.  
778 *Geoderma* 2016; 270: 68-75.

779 Takahashi Y, Minamikawa R, Hattori KH, Kurishima K, Kihou N, Yuita K. Arsenic  
780 Behavior in Paddy Fields during the Cycle of Flooded and Non-flooded Periods.  
781 *Environmental Science & Technology* 2004; 38: 1038-1044.

782 Tokunaga S, Hakuta T. Acid washing and stabilization of an artificial  
783 arsenic-contaminated soil. *Chemosphere* 2002; 46: 31-38.

784 Tournassat C, Charlet L, Bosbach D, Manceau A. Arsenic(III) oxidation by birnessite

785 and precipitation of manganese(II) arsenate. *Environmental Science &*  
786 *Technology* 2002; 36: 493.

787 Van HS, Swennen R, Vandecasteele C, Cappuyns V. Solid Phase Speciation Of  
788 Arsenic By Sequential Extraction In Standard Reference Materials And  
789 Industrially Contaminated Soil Samples. *Environmental Pollution* 2003; 122:  
790 323-42.

791 Villen-Guzman M, Gomez-Lahoz C, Garcia-Herruzo F, Vereda-Alonso C, Paz-Garcia  
792 JM, Rodriguez-Maroto JM. Specific Energy Requirements in Electrokinetic  
793 Remediation. *Transport in Porous Media* 2017: 1-11.

794 Wan X, Lei M, Chen T. Cost-benefit calculation of phytoremediation technology for  
795 heavy-metal-contaminated soil. *Science of the Total Environment* 2016; s  
796 563–564: 796-802.

797 Weber FA, Hofacker AF, Voegelin A, Kretzschmar R. Temperature dependence and  
798 coupling of iron and arsenic reduction and release during flooding of a  
799 contaminated soil. *Environmental Science & Technology* 2010; 44: 116-122.

800 Wenzel WW, Kirchbaumer N, Prohaska T, Stingeder G, Lombi E, Adriano DC.  
801 Arsenic fractionation in soils using an improved sequential extraction procedure.  
802 *Analytica Chimica Acta* 2001; 436: 309-323.

803 Williams PN, Lei M, Sun G, Huang Q, Lu Y, Deacon C, et al. Occurrence and  
804 partitioning of cadmium, arsenic and lead in mine impacted paddy rice: Hunan,  
805 China. *Environmental Science & Technology* 2009; 43: 637.

806 Wu B, Liao XY, Chen TB. Comparison of five methods for fractionation of  
807 calcareous soil contaminated with arsenic. *Acta Scientiae Circumstantiae* 2006;  
808 26: 1467-1473.

809 Xu X, Chen C, Wang P, Kretzschmar R, Zhao FJ. Control of arsenic mobilization in  
810 paddy soils by manganese and iron oxides. *Environmental Pollution* 2017; 231:  
811 37-47.

812 Yamaguchi N, Nakamura T, Dong D, Takahashi Y, Amachi S, Makino T. Arsenic  
813 release from flooded paddy soils is influenced by speciation, Eh, pH, and iron  
814 dissolution. *Chemosphere* 2011; 83: 925-932.

815 Ying SC, Kocar BD, Fendorf S. Oxidation and competitive retention of arsenic  
816 between iron- and manganese oxides. *Geochimica Et Cosmochimica Acta* 2012;  
817 96: 294-303.

818 Yu P, Zhang X, Wang D, Wang L, Ma Y. Shape-Controlled Synthesis of 3D  
819 Hierarchical MnO<sub>2</sub> Nanostructures for Electrochemical Supercapacitors. *Crystal*  
820 *Growth & Design* 2013; 9: 528-533.

821 Z Y, W Q, F W, M L, D W, Z S. Effects of manganese oxide-modified biochar  
822 composites on arsenic speciation and accumulation in an indica rice (*Oryza*  
823 *sativa* L.) cultivar. *Chemosphere* 2017; 168: 341-349.

824 Zhang RH, Li ZG, Liu XD, Wang BC, Zhou GL, Huang XX, et al. Immobilization  
825 and bioavailability of heavy metals in greenhouse soils amended with rice  
826 straw-derived biochar. *Ecological Engineering* 2017; 98: 183-188.

827 Zhang WX. Nanoscale Iron Particles for Environmental Remediation: An Overview.  
828 *Journal of Nanoparticle Research* 2003; 5: 323-332.

829 Zhao FJ, Ma Y, Zhu YG, Tang Z, Mcgrath SP. Soil contamination in China: current  
830 status and mitigation strategies. *Environmental Science & Technology* 2015; 49:  
831 750.

832 Zheng MZ, Cai C, Hu Y, Sun GX, Williams PN, Cui HJ, et al. Spatial distribution of  
833 arsenic and temporal variation of its concentration in rice. *New Phytologist* 2011;  
834 189: 200.

835